

# Picometer level displacement metrology with digitally enhanced heterodyne interferometry

Glenn de Vine,<sup>1</sup> David S. Rabeling,<sup>1</sup> Bram J. J. Slagmolen,<sup>1</sup> Timothy T-Y. Lam,<sup>1</sup> Sheon Chua,<sup>1</sup> Danielle M. Wuchenich,<sup>1</sup> David E. McClelland,<sup>1</sup> and Daniel A. Shaddock<sup>1,2</sup>

<sup>1</sup>*Centre for Gravitational Physics, College of Physical Sciences, The Australian National University, Canberra, ACT 0200, Australia*

<sup>2</sup>*Jet Propulsion Laboratory, California Institute of Technology, Pasadena, CA 91109*  
[daniel.shaddock@jpl.nasa.gov](mailto:daniel.shaddock@jpl.nasa.gov)

**Abstract:** Digitally enhanced heterodyne interferometry is a laser metrology technique employing pseudo-random codes phase modulated onto an optical carrier. We present the first characterization of the technique's displacement sensitivity. The displacement of an optical cavity was measured using digitally enhanced heterodyne interferometry and compared to a simultaneous readout based on conventional Pound-Drever-Hall locking. The techniques agreed to within  $5 \text{ pm}/\sqrt{\text{Hz}}$  at 1 Hz, providing an upper bound to the displacement noise of digitally enhanced heterodyne interferometry. These measurements employed a real-time signal extraction system implemented on a field programmable gate array, suitable for closed-loop control applications. We discuss the applicability of digitally enhanced heterodyne interferometry for lock acquisition of advanced gravitational wave detectors.

© 2009 Optical Society of America

**OCIS codes:** (120.0120) Instrumentation, measurement, and metrology; (040.2840) Heterodyne detectors.

---

## References and links

1. N. Bobroff, "Recent advances in displacement measuring interferometry," *Meas. Sci. Technol.* **4**, 907 (1993).
2. D. A. Shaddock, "Digitally enhanced heterodyne interferometry," *Opt. Lett.* **32**, 3355-3357, (2007).
3. O. Lay, S. Dubovitsky, D. A. Shaddock, and B. Ware, "Coherent range-gated laser distance metrology with compact optical head," *Opt. Lett.* **32**, 2933-2935 (2007).
4. R. W. P. Drever, J. L. Hall, F. V. Kowalski, J. Hough, G. M. Ford, A. J. Munley, and H. Ward, "Laser phase and frequency stabilization using an optical resonator," *Appl. Phys. B* **31**, 97, (1983).
5. O. Lay, Private Communication (2008).
6. See for example <http://www.ligo.caltech.edu/advLIGO/> or A. Weinstein for the LSC, "Advanced LIGO optical configuration and prototyping effort," *Class. Quantum Grav.* **19**, 1575-1584, (2002).
7. Y. Aso, M. Ando, K. Kawabe, S. Otsuka, and K. Tsubono, "Stabilisation of a Fabry-Perot interferometer using a suspension-point interferometer," *Phys. Lett. A* **327**, 18, (2004).
8. B. J. J. Slagmolen, G. de Vine, D. S. Rabeling, K. McKenzie, A. J. Mullavey, D. A. Shaddock, D. E. McClelland, M. Evans, and Y. Aso, "Advanced LIGO arm cavity pre-lock acquisition system," <http://www.ligo.caltech.edu/docs/T/T080139-00.pdf> (2008).

## 1. Introduction

Optical metrology is a key enabling technology for a broad range of scientific applications such as telescope control, fiber optic sensors, precision spacecraft positioning and gravitational wave detection. Heterodyne interferometry [1] is a widely used technique for sub-nanometer displacement metrology. Digitally enhanced heterodyne interferometry (DI) [2] is a new technique that augments conventional heterodyne interferometry with digital modulation-demodulation to provide robust, high-sensitivity displacement measurements. DI employs pseudo-random noise (PRN) phase modulation to isolate interferometric signals based on their delay. This signal isolation, arising from the autocorrelation properties of the PRN code, enables both rejection of spurious signals (e.g. from scattered light) and multiplexing capability using a single metrology system. Previous work [3] focused on the technique's measurement linearity and demonstrated a cyclic error of 1.1 nm. In this article we characterize DI's displacement sensitivity by comparing it to Pound-Drever-Hall (PDH) [4] locking of an optical cavity.

In this paper, DI is used to measure the cavity displacement by detecting the light transmitted through the cavity. The cavity displacement can be inferred from the phase difference between the single-pass and the first round-trip beams. Previous work employed reflection-based DI measurements. In a reflection configuration, minimizing cross-talk between the respective signals requires the use of low reflectivity mirrors to approximately match the electric field amplitudes. For highly reflective optical components, such as those used in optical cavities, the reflection from the first mirror will dominate the signals at the photodetector. The transmitted signals, however, will have approximately equal amplitudes and thus transmission-based DI measurements are preferred for highly reflective optical components.

Consider the optical layout shown in Fig. 1, where two partially reflecting mirrors, M1 and M2, form an optical cavity. A beamsplitter divides the laser output field into a local oscillator beam and a probe beam. The local oscillator is frequency-shifted by an acousto-optic modulator (AOM), providing a heterodyne signal with frequency  $f_h$  at the photodetector. A PRN code generator drives an electro-optic modulator (EOM) to produce either a zero or  $\pi$  phase shift on the probe beam before it is directed toward mirrors M1 and M2. The transmitted light is recombined with the local oscillator and the interference signal is measured by the photodetector.

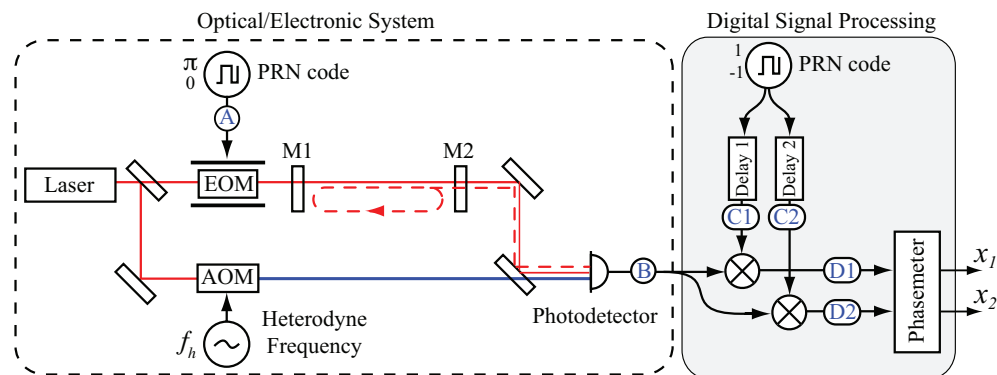


Fig. 1. Digital Interferometer for monitoring displacements of two mirrors, M1 and M2. Signals are isolated by matching the decoding delays to the optical delays. Signals measured at points A, B, C1, C2, D1, and D2 are shown in Table 1.

The key difference between DI and conventional heterodyne interferometry is the PRN phase modulation. With no PRN modulation, the heterodyne signal at the photodetector is determined by the vector sum of the single-pass electric field and all subsequent round-trip electric fields.

The phase of the individual fields can not be recovered. With the PRN modulation imposed, the respective signals will possess a time-varying phase shift unique to their time of flight from the EOM, allowing them to be individually recovered in signal processing.

Table 1 shows the effect of the PRN encoding and decoding on the measured signals. For clarity the following explanation considers only the encoding and decoding of the single-pass signal. The first row shows the signal at the photodetector in a conventional heterodyne interferometer (a beat-note at  $f_h$ ). With digital interferometry, the PRN code (A) randomly inverts the heterodyne signal at the photodetector producing a chopped sine wave (B). In the processing channel for monitoring the single-pass phase shift, the photodetector output is multiplied by the PRN code with a matching delay (C1), to recover the original heterodyne signal (D1). Optical path length information is contained in the phase of this heterodyne signal. The right-hand column shows the signals obtained using a mismatched decoding delay (C2); in this case the signal is randomly re-inverted (D2) and appears in the measurement as a broadband noise floor. This broadband noise can be strongly rejected by appropriate filtering and averaging in the phasemeter. This demonstrates that by adjusting the decoding delay, we can selectively isolate signals based on their total optical/electronic delay.

Table 1. Signals from single-pass beam with matched (middle column) and unmatched (right column) decoding delays. Signals A, B, C1, C2, D1, D2 correspond to the measurement points in Fig. 1.

	Matched decoding delay	Mismatched decoding delay
Conventional heterodyne		
PRN encoding	(A)	(A)
Detected single-pass signal	(B)	(B)
PRN decoding	(C1)	(C2)
Decoded output	(D1)	(D2)

The shot noise level of DI is equivalent to the shot noise level of conventional heterodyne interferometry. Like other broadband noise (e.g. electronic noise), the shot noise level is unaffected by the digital decoding due to the random nature of shot noise and its lack of correlation with the PRN code. The single sided amplitude spectral density of phase noise due to shot noise for each decoded output is given by,

$$\delta\phi_{sn} = \sqrt{\frac{h\nu}{P}} \quad \text{rad}/\sqrt{\text{Hz}} \quad (1)$$

where  $P$  is the detected optical power of the signal,  $h$  and  $\nu$  Planck's constant and the optical frequency respectively. For round-trip measurements this can be converted to displacement noise by multiplying by  $\lambda/4\pi$  (or  $\lambda/2\pi$  for one-way measurements). Conventional heterodyne interferometry measurements, however, are often limited by technical noise sources, such as spurious interference, well above the shot noise limit.

## 2. Displacement sensitivity characterization

The experimental layout is presented in Fig. 2 showing a local oscillator (LO) laser and carrier laser. The lasers were Nd:YAG Non Planar Ring Oscillators (one Innolight Mephisto and one Lightwave model 126) operating at 1064 nm. The LO laser was offset phase locked to the carrier

laser to provide the heterodyne frequency for the DI measurement (this phase locking replaced the AOM of Fig. 1). The carrier laser had two functions: to act as the probe beam for the DI measurement and to implement the PDH sensing system. Using the same laser for the DI and PDH measurements provides a large common mode rejection of laser frequency noise.

The optical cavity under test was 3.75 m long with a finesse  $\mathcal{F} \approx 30$  mounted on an optical bench in air. Both cavity mirrors had a power reflectivity of 90%, with a flat input coupler and a 6 m radius of curvature output coupler.

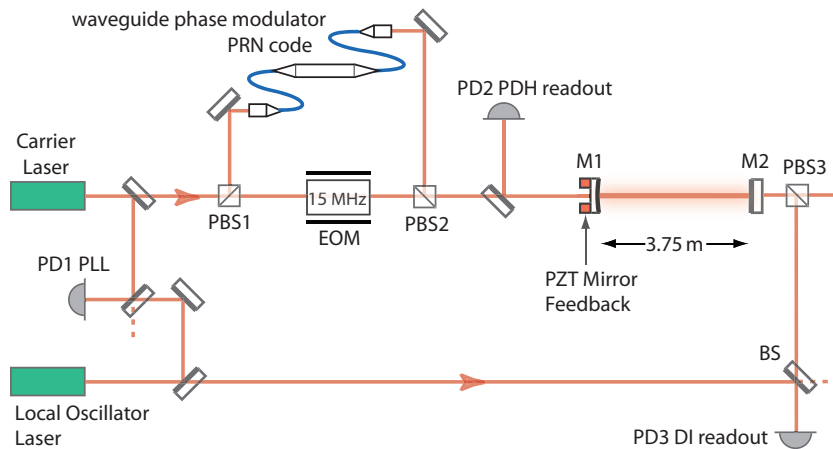


Fig. 2. Simplified experimental layout of digital interferometry transmission technique for displacement sensitivity measurements.

The carrier laser light was divided into the DI probe beam and PDH beam at PBS1. These beams were individually modulated with their respective signals before being sent to the optical cavity. The DI probe beam was phase modulated by a fiber coupled EOSpace phase modulator (model PM-0K5) with an 80 MHz PRN code to provide a 0 or  $\pi$  radians phase shift. The cavity length was chosen to equal the wavelength of the PRN code ( $c/80 \text{ MHz}=3.75 \text{ m}$ ). Although not strictly necessary, matching the optical component separation to an integer number of PRN wavelengths simplifies the digital signal processing by allowing integer delays to be used in the decoding. The PRN code was a maximal length sequence of length  $n = 2^{14} - 1 = 16383$  chips.

The PDH beam was phase modulated at 15 MHz by a resonant NewFocus EOM (model 4003). The DI probe beam and the PDH beams were then recombined on PBS2, with orthogonal polarizations and directed into the optical cavity. The signal reflected from the cavity was detected at photodiode PD2 and the PDH signal was demodulated at 15 MHz and low-pass filtered to generate the PDH error signal. This error signal was fed into an analog controller which sent the correction signal back to the PZT on M1 to keep the cavity on resonance. The locking bandwidth for this control system was approximately 150 Hz, limited by the PZT-mirror mechanical resonance.

After transmission through the cavity the PRN phase-modulated field was separated from the PDH carrier field using a polarizing beam splitter, PBS3. PBS3 was needed to avoid saturating photodetector PD3 with the PDH beam transmitted through the cavity on resonance. PBS3 reduced the power of the PDH beam at PD3 to 3.2 W. The DI probe beam was interfered with the local oscillator and detected on photodiode PD3. The LO power incident on PD3 was 4.3 mW, with 29 nW from the DI probe beam. The signal from PD3 was digitized by an 80 MHz, 15 bit analog to digital converter (Maxim 1427). A Field Programmable Gate Array (FPGA)

decoded and measured the phase of the signals in real-time using a National Instruments PXI board (NI PXI-7833R). This real-time signal extraction is an improvement over previous work [3], which recorded the photodetector output using a digital oscilloscope and performed the PRN decoding and phase measurement off-line in software.

The displacement of the cavity can be inferred from the phase difference between the straight through beam and the beam that experiences one (or more) round-trips through the cavity. The decoding delay for the single-pass channel was selected to include the total electronic-optical-electronic delay of the PRN code from the FPGA output to the FPGA input. The round-trip channel decoding delay included this single-pass delay, plus an additional delay to account for the round-trip pass(es) in the optical cavity. After decoding, the phase of each channel was extracted using a phasemeter based on a digital phase locked loop implemented on the same FPGA. The difference of these two phase measurements was recorded to provide an out-of-loop measurement of the cavity displacement.

### 3. Results

The separation of the cavity mirrors can be inferred from the phase difference between beams making  $j$  and  $k$  round trips,

$$\delta L = \frac{\lambda}{2\pi} \frac{(\phi_j - \phi_k)}{2(j - k)} \quad (2)$$

where  $j$  and  $k$  are integers and  $\phi_j$  denotes the phase of the beam (in radians) that has experienced  $j$  round-trips through the cavity. The denominator is needed for normalization because the accumulated phase shift is proportional to the number of traversals between the mirrors. Figure 3 presents the root power spectral density of the DI displacement measurement. This measurement was made using the 2nd and 6th round-trip beams ( $j = 6$ ,  $k = 2$  in Eq. 2). A displacement sensitivity of approximately  $5 \text{ pm}/\sqrt{\text{Hz}}$  was achieved at frequencies above 1 Hz. The roll-off above 100 Hz is due to the transfer function of the phasemeter and does not signify improved displacement noise. The phasemeter's digital phase locked loop unity gain frequency was  $\sim 100$  Hz therefore it did not faithfully reproduce phase fluctuations above this frequency.

There are several candidate error sources to account for the increased noise below 1 Hz.  $1/f$  noise in the PDH system, in particular the mixer and analog controller, could potentially degrade the PDH locking over long time scales. To rule this out we performed an in-loop measurement using a digital implementation of the mixer and low-pass filter, which should be free of  $1/f$  analog electronic noise. The photodiode output was split into two signals. One signal was used by the analog PDH control system in the usual way. The second signal was digitized at 40 MHz and demodulated and low-pass filtered inside the FPGA, providing a digital error signal for analysis. Figure 4 shows a comparison of the spectral densities of the DI measurement (A) and the digital PDH in-loop measurement (B).

This plot shows that the low frequency noise of the digital PDH signal is well below the DI measurement noise floor indicating that the digital and analog PDH sensors agree very well. From this we conclude that the noise in the analog electronics used to implement the PDH locking does not limit the measurement at low frequencies. However, this test does not rule out errors in the PDH system due to residual amplitude modulation produced by imperfections in the phase modulation process. This error would be common to both analog and digital PDH systems and would not be revealed in the difference signal.

Another candidate for the excess low frequency noise is contamination of the DI measurement by the PDH beam leaking through the cavity. Recall that even after most of the PDH beam is rejected by PBS3, its power is 100 times larger than the total detected DI probe beam power. This total probe beam power is made up of contributions from many cavity round-trips and

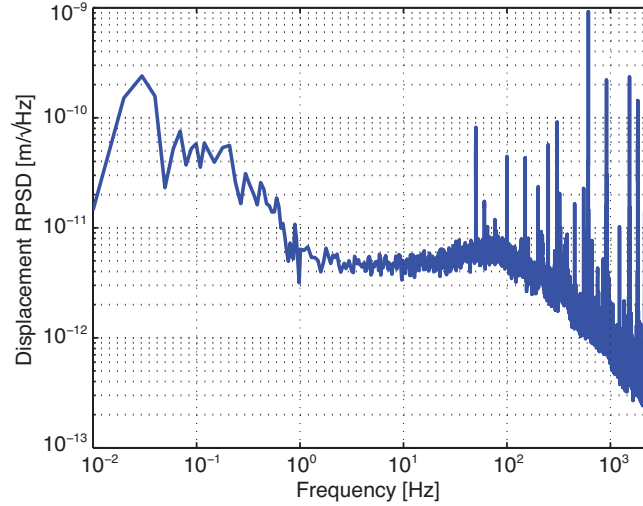


Fig. 3. Spectral density of the DI measurement of cavity displacement when the cavity is locked using PDH locking. Spectral density averaged for clarity (3x for  $0.1 > f > 1$  Hz, and 10x for  $f > 1$  Hz). note: The roll-off above 100 Hz is due to the transfer function of the phasemeter.

the power of any individual contribution is at least a factor of 5 lower still (for cavity mirror reflectivities  $R=0.9$ ). This PDH beam will interfere with the LO to produce a beat note at the heterodyne frequency. The suppression of this spurious beat note by the decoding stage is finite and some level of contamination of the DI measurement can be expected. The displacement error due to this contamination will be of order,

$$\delta L_{PDH} \sim \frac{\lambda}{2\pi} \sqrt{\frac{P_{PDH}}{P_{DI}}} \frac{\sqrt{2}\delta\theta}{2(j-k)\alpha} \quad (3)$$

where  $P_{PDH}$  and  $P_{DI}$  are the powers of the PDH beam and DI beam on detector PD3 and  $\alpha$  is the suppression factor of the PRN decoding. The factor of  $\sqrt{2}$  in the numerator is needed because the displacement is inferred from the difference of two phase measurements, i.e. the  $j$ th and  $k$ th round-trips. The factor of  $2(j-k)$  in the denominator converts from phase difference over multiple round-trips to the single pass phase shift.  $\delta\theta$  is the fluctuation in relative phase of the PDH and PRN beams (e.g. through path length changes in the optical fiber or phase modulators between PBS1 and PBS2). These path lengths were neither measured nor controlled in our experiment. We expect that fluctuations of the order of a wavelength ( $\delta\theta \sim 2\pi$ ) were present over time scales of 100 seconds.

The suppression factor  $\alpha$  can be estimated from measurements of the crosstalk between the 0th and 4th round-trips through the cavity. With the PDH beam blocked at the EOM, we scanned the cavity length by driving the M1 PZT with a 1 Hz triangle wave. The cavity displacement should phase shift all beams that undergo at least one round-trip, but it should be absent from the phase of single-pass beam. Figure 5 presents time-domain traces of DI measurements of the single-pass and 4th-round-trip signals.

The phase of the 4th-round-trip field clearly shows the triangular scan driving the cavity mirror PZT. For the single-pass demodulation, almost no triangular signal can be seen, indicating low cross-talk between signals. The root power spectral density of these signals shown in Fig.

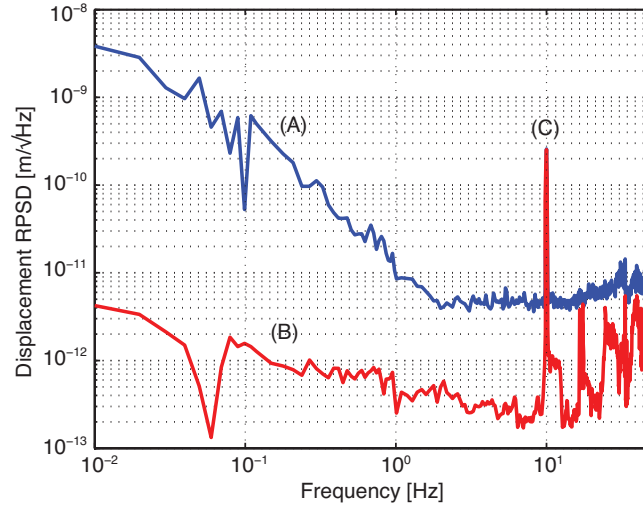


Fig. 4. Comparison of DI readout (A) and digital implementation of PDH readout (B) with the cavity locked using the analog PDH system. The feature (C) is a calibration peak used to scale the digital PDH readout. The lower noise level of (B) indicates good agreement of analog and digital PDH systems and rules out analog electronic noise in the mixer and controller as the limitation of the DI measurement.

6 exhibits a suppression factor  $> 1000$  for the fundamental 1 Hz peak (the other peaks are the Fourier harmonics of the triangle wave drive frequency). The background noise is higher than in Fig's 3 and 4 as it is not a differential measurement and thus includes the optical path noise of the input fibers/modulators relative to the LO phase.

Substituting  $\alpha = 1000$  into Eq. 3 with  $(j - k) = 4$  gives,

$$\delta L_{PDH} \sim \delta\theta \times 670 \text{ pm} \quad (4)$$

Equation (4) implies that an optical path length noise of only  $50 \text{ nm}/\sqrt{\text{Hz}}$  (equivalent to  $\delta\theta \sim 0.3 \text{ rad}/\sqrt{\text{Hz}}$ ) in the non-common path between PBS1 and PBS2 would account for the  $200 \text{ pm}/\sqrt{\text{Hz}}$  maximum noise level shown in Fig. 3. Note that this noise source is introduced by the PDH beam used to characterize the DI performance and is not inherent to the DI measurement.

Another potential source of low frequency noise in the DI readout is alignment fluctuations of the DI input beam relative to the cavity. Imperfect polarization states in the DI modulator could also introduce a measurement error under some circumstances [5]. This error, caused by the interference with the unwanted polarization mode, can be mitigated by using a polarizing electro-optic modulator.

One of the key advantages of DI measurements for many applications is the linearity and large range of the readout. This is illustrated by Fig. 3 which shows a comparison of the DI and PDH readouts as the cavity is scanned over more than 1 free spectral range (FSR).

Analysis of this data indicates that PDH and digital interferometry agree on the cavity's FSR down to an error of 0.6%. The data shows that 1 FSR measured by PDH equals 1.0063 cycles measured by digital interferometry. This error could be due to polarization dependent phase shift in the optical cavity. The 3.75 m cavity was folded to fit on the optical bench and the PDH and DI beams were orthogonally polarized inside the cavity.

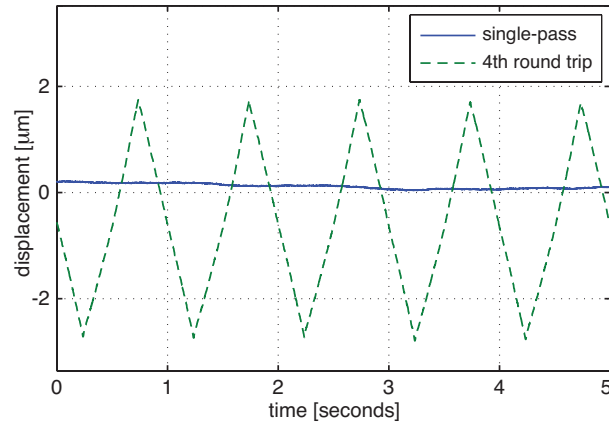


Fig. 5. Single-pass and 4th-round-trip DI measurements when the cavity length is scanned. The cavity length change appears strongly in the phase measurement of the 4th-round-trip but not in the single-pass phase measurement.

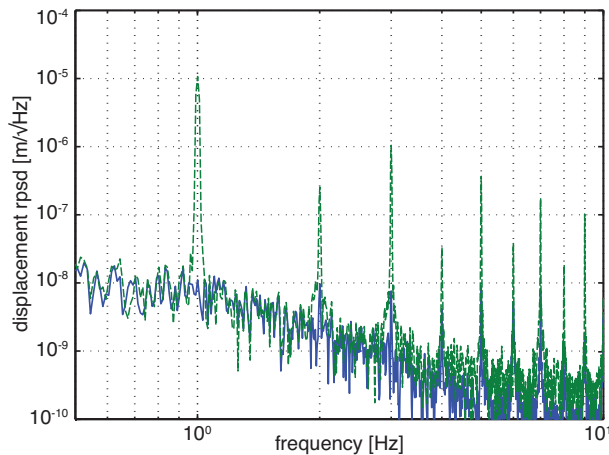


Fig. 6. Root power spectral density of data from Fig. 5. The ratio of the 1 Hz scan signal sets an upper bound on the crosstalk between channels at less than  $10^{-3}$  ( $\alpha > 1000$ ).

#### 4. Discussion

One possible application for digital interferometry is to aid in the lock acquisition of next generation interferometric gravitational wave detectors, such as Advanced LIGO [6]. The residual motion of the Advanced LIGO test masses, predicted to be up to  $100 \text{ nm}/\sqrt{\text{Hz}}$ , combined with a more sophisticated optical configuration makes lock acquisition a challenging problem. A suspension point interferometer [7] has been proposed to reduce this initial motion by a factor of 10 to 100 to improve the lock acquisition process. An alternative solution is to use DI in a closed-loop control system to reduce the initial mirror motion [8]. DI's large dynamic range ( $\gg 1 \text{ m}$ ) and ability to isolate the LIGO arm cavity longitudinal degrees of freedom are well suited to such an application. A lock acquisition system for Advanced LIGO requires a displacement sensitivity of better than  $1 \text{ nm}/\sqrt{\text{Hz}}$  below 1 Hz and approximately  $10 \text{ pm}/\sqrt{\text{Hz}}$

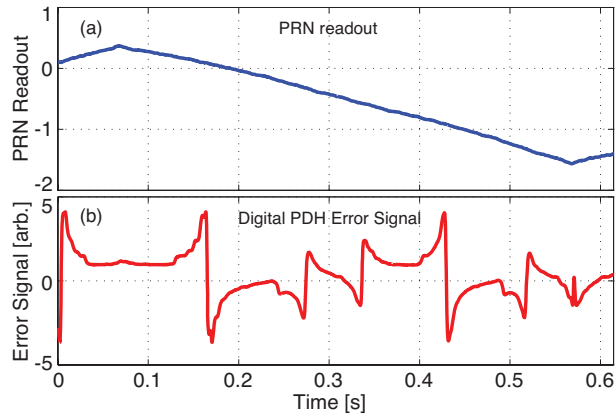


Fig. 7. Comparison of (a) DI and (b) PDH signals as the cavity length is scanned over more than one FSR. The techniques differ by 0.6% on the FSR. 1 FSR measured by PDH equal to 1.0063 cycles measured by digital interferometry. Note that the DI readout remains linear over the entire FSR.

above 1 Hz. The more stringent requirement above 1 Hz derives from the need to limit actuation at high frequencies [8].

The DI measurements presented here meet this sensitivity requirement. However, for application to Advanced LIGO it will be critical to understand the effect of alignment fluctuations on the DI measurement, and in particular how such errors scale with interferometer length. Another significant challenge in applying DI to Advanced LIGO is preventing measurement contamination by the main science laser. The arm cavities will have a circulating power of up to 500 kW when locked to the laser frequency. Approximately 1 W of light power will be transmitted through the end mirror. For a 200 mW DI laser input power, approximately 1 nW will be transmitted through the arm cavity end mirror. Under these conditions, the science laser to DI laser power ratio will be approximately  $10^9$ , significantly greater than in the experiment conducted here. Isolating the DI signal from the science laser at the detection end will be important in reducing this ratio, thereby reducing the sensitivity noise floor. We propose frequency shifting the DI laser with respect to the science laser. A frequency offset of order 1 GHz would move the science laser-LO beat note outside of the bandwidth of the photodetector. A large frequency shift would also allow the science laser to be attenuated before the photodetector, e.g. by spatially separating the DI and science lasers with a diffraction grating or short cavity. In combination with other isolation methods, such as cross-polarizing the science and DI lasers and using polarization optics before detection, it should be possible to reduce the contamination to manageable levels.

## 5. Conclusion

Digital interferometry was used to make displacement measurements of a Fabry-Perot cavity. Comparison with an independent PDH locking system gave an upper limit to the DI displacement sensitivity of  $5 \text{ pm}/\sqrt{\text{Hz}}$  at frequencies above 1 Hz. Excess noise at low frequencies at a level of  $200 \text{ pm}/\sqrt{\text{Hz}}$  can be accounted for by contamination of the DI measurements by the PDH system used for characterization. A real-time signal extraction system suitable for closed-loop control was implemented on a single FPGA including PRN decoding and a phasemeter. DI's displacement sensitivity and large dynamic range make it a suitable candidate for lock

acquisition in advanced gravitational wave detectors.

### **Acknowledgments**

The authors thank Brent Ware and Oliver Lay for useful discussions. This research was supported by the Australian Research Council. Part of this research was performed at the Jet Propulsion Laboratory, California Institute of Technology, under contract with the National Aeronautics and Space Administration.